



Voltage Oriented Control Approach in Smart Microgrids with Large Scale Energy Storage Integration

Felicidade Pemba Kinzo Garcia¹, Atanda Kamoru Raji¹, Khaled M Abo-Al-Ez²

¹Cape Peninsula University of Technology, Bellville 7535, Western Cape, South Africa,

²Engineering Management, University of Johannesburg, Johannesburg, South Africa

Email: 217297188@mycput.ac.za¹, raja@cput.ac.za²
khaleda@uj.ac.za³

Received 01 April 2024; revised 29 April 2024; accepted 10 June 2024

Abstract

Microgrids refer to small-scale power systems formed from distributed generations, storage devices, and loads, operating synchronised with integrated power electronic units. Since the power supply and the microgrid load are unstable, including energy storage may allow power balance while assuring the microgrid's suitable predictability. Energy storage can deal with the microgrid's unpredictability. Simultaneously, the grid can control the energy storage and the distributed generations with the power dispatching so that the microgrid can alleviate the grid pressure. The system includes interfacing power converters allowing controllable power flow from sources to the loads. This paper considers microgrids, including wind turbines, large-scale energy storage and DC load. The aim is to model a voltage-oriented control scheme for a three-phase PWM rectifier interfacing the wind turbine, the DC load, and the energy storage. The modelling and simulation are performed using the Simulink environment. Microgrids, composed of distributed generation, energy storage, and loads, offer enhanced resilience and energy management. However, the intermittent of renewable sources like wind requires effective control strategies to maintain stability. Large-scale energy storage can mitigate these fluctuations, ensuring a balanced and predictable power supply. This paper presents a Voltage-Oriented Control (VOC) approach for integrating wind turbines, large-scale energy storage, and a DC load within a microgrid. The proposed control scheme uses a three-phase PWM rectifier to interface these components, optimizing power flow and maintaining stable voltage. The VOC approach ensures efficient energy management, regulating voltage levels while balancing power between the renewable generation, storage, and load. Modeling and simulation are performed in Simulink, demonstrating the system's ability to stabilize voltage and efficiently dispatch energy. The results show that the VOC strategy enhances microgrid performance, improves power quality, and alleviates pressure on the main grid. This approach provides a reliable and predictable energy supply, improving microgrid stability and supporting grid interaction.

Keywords: *Energy storage, Control System, PWM rectifier, renewable microgrid, wind turbine.*

Introduction

During the last two decades, electricity demand has become higher due to industrial progress and population growth worldwide. An investigation conducted on the power consumption and economic development of 274 cities reveals that these cities need to minimise their energy utilisation by more than 25%. The study concluded that if no mitigation actions are taken, the energy use will rise by more than three times between 2005 and 2050 (Thorpe, 2015). Furthermore, with suitable urban design and transport rules, the future increase in urban energy would be limited to 150 000 TWh in 2050, thus decreasing the potential of climate change. Moreover, these cities would need to implement more policies to reduce urban greenhouse gas emissions (Thorpe, 2015). The questions come up in how these issues will be solved, what kinds of energy sources and technologies will be used to meet such amount (Stephen, 2017).

Today's electricity market still relies on fossil fuel, including coal, gas, and oil, to meet the load demand. However, these energy sources are disadvantageous, as they can release an important quantity of carbon dioxide into the atmosphere, potentially increasing the risks of global warming. Moreover, it is notable that those sources are running out and will probably cause an energy shortage in the next three decades (Ellabban et al., 2014; Stephen, 2017). Other energy technologies, such as wind, solar, hydro, biomass, etc., have been developed to address the presented issues. The target is to keep on developing these renewable technologies until energy sources based on fossil fuels are replaced (Stephen, 2017)

The main issues when dealing with these renewable technologies are their variability and reliability caused by meteorological factors. This renewable power instability also challenges their integration into the grids. Due to these issues, research efforts have been made to determine suitable technologies for renewable energy integration in the power network.

In this context, the microgrid concept appears to be the appropriate solution for integrating renewable power into the grid. Microgrids refer to small-scale power systems formed from distributed generations, storage systems, and groups of loads, operating in synchronised mode with integrated power electronics units; they can operate in islanded mode or connected to the main power grids (Arbab-Zavar et al., 2019; Planas et al., 2015). The ability to work in both grid-connected and off-grid modes increases the power quality, energy security, and reliability to the end-users (Planas et al., 2015).

Microgrids can be designed to feed both AC and DC loads, but most microgrids generate AC power to facilitate their interaction with the grids. However, DC microgrids are gaining more attention because of the power nature of technologies such as photovoltaic panels, fuel cells, batteries, and supercapacitors and the increasing presence of DC loads. DC microgrids present significant benefits over AC microgrids; these benefits include the absence of harmonics and reactive power. Additionally, DC microgrids are more efficient and straightforward as they do not have multi-stage conversions from AC to AC via DC (ArbabZavar et al., 2019).

Besides power sources such as photovoltaic panels and fuel cells, AC renewable generators can also be used in DC microgrids. In such a case, they require an AC to DC-conversion through a rectifier. This study considers a DC microgrid composed of an AC wind generator, a three-phase PWM rectifier, an energy storage system, and a DC load. Including energy storage may allow power balance while assuring suitable microgrid predictability. Similarly, the grid can control the energy storage and the distributed generations with the power dispatching so that the microgrid can alleviate the grid pressure. The system includes interfacing power converters allowing controllable power flow from sources to the loads.

Several studies on the control of PWM rectifiers have been carried out. Frisfelds and Krievs (Frisfelds and Krievs, 2019) presented the design of a low voltage three-phase PWM bidirectional converter. The objective was to achieve a low harmonic distortion to meet IEEE 519-1992. A control algorithm was developed for the control of the PWM rectifier. A similar study was conducted by Kondylis et al. (Kondylis et al., 2017). The authors developed a control system to regulate the power flow from the primary source to the batteries to keep the systems' variables such as frequency and voltage within reasonable limits. Li et al. (Qiang et al., 2015) proposed a hybrid system's control scheme, including wind, PV, and storage systems for microgrids; this system is based on bidirectional converters operating in both modes rectifier and inverters. The approach was developed to improve electrical energy quality. The systems are composed of a PI controller and neural network. The authors used the wind speed to 10 m/s, rotor diameter of 1.56 m, the turbulence intensity of 12%. The wind generator was based in PMSG; the results showed that the system was advantageous. The converter voltage generates a total harmonic distortion (THD) of 5.7%. Compared to this study, the wind speed was 13 m per second, the rotor diameter was 33.05 m, and the total harmonic distortion was 13.54%. Both values of the THD are within the applicable standard and adequate for the system. Another approach was developed by Davood et al. (Khaburi and Nazempour, 2010). The study was based on a PWM rectifier's design and simulation connected to a PMSG for a micro wind turbine. The study's purpose was to present a model for a voltage source rectifier connected to the generator in the

microturbine. The authors used the virtual flux direct power control strategy (VF-DPC). In the configuration, the DC-bus voltage is controlled by regulating the active power.

Similarly, Yusoff et al. (Yusoff et al., 2017) proposed using the VF-DPC to improve the control method in contrast to the conventional direct power control strategy DPC for the front-end three-phase PWM rectifier converter. The parameters used in the study are tabulated in Table 5. Frisfelds and Krievs (Frisfelds and Krievs, 2019) implemented the control of rectifier with a synchronous rotating dq frame to control load current in dq-axis components and control the active and reactive power individually to set the DC-link voltage constant during the dynamic load changes. The results also showed that the designed rectifier system is stable, and the grid current harmonic in both the low and the high-frequency ranges is low (Frisfelds and Krievs, 2019). A similar study was implemented by Kondylis et al. (Kondylis et al., 2017). They proposed a control system based on voltage-oriented control strategy (VOC); the controller generates enough PWM pulses to a converter to monitor the activities of a stand-alone network and manage the active and reactive power flows between the storage systems and the grid as well as to provide an acceptable power quality. The result showed an adequate voltage quality in all buses, and the harmonic distortion was set within limits. This study's focus was the control of frequency in a stand-alone mode powered only by wind energy. The results showed that the control was achieved with the master controller's suitable setting that determined the proper energy flows within the system and kept the frequency within the required boundaries (Kondylis et al., 2017).

The present study aims to develop a control scheme for a three-phase PWM rectifier interfacing the wind turbine, a DC load, and an energy storage unit. This study's main contribution is to present a detailed wind turbine DC microgrid model based on Simulink. The rest of the paper is as follows. The next section is dedicated to system description modelling and control. The third section discusses the results and compares them with other studies, and the fourth section deals with the conclusion. **System Modelling**

As depicted in Figure 1, the adopted DC microgrid consists of a permanent magnet synchronous generator (PMSG) wind turbine connected to a PWM rectifier supplying an energy storage device and a DC load.

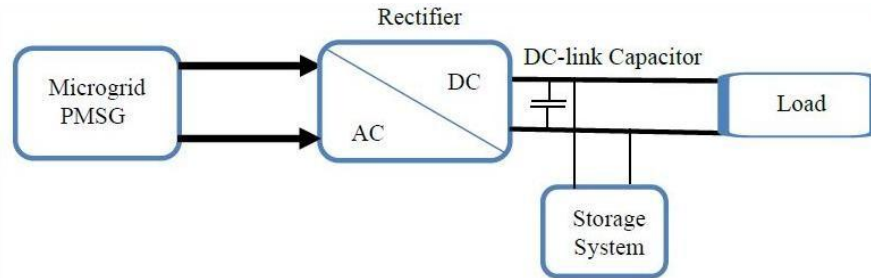


Figure 1 System Layout

Permanent Magnet Synchronous Generator (PMSG)

A PMSG offers a high-efficiency power conversion from mechanical to electrical power. In this type of generator, the excitation field is given by a permanent magnet rather than a coil. It is referred to as a synchronous generator because the rotor and the magnetic field rotate at the same speed. A shaft generates the magnetic field mounted permanent magnet mechanism and the current is induced into the stationary armature (Binder and Schneider, 2005). Two types of PMSGs can be distinguished namely salient rotor and round rotor. This study considers a round rotor generator. The PMSG modelling equations are expressed as follows (Caixeta et al., 2014):

$$\sqrt{6} V_{nom} \Phi_{nom} = \frac{1}{\omega_{nom}} \quad (1)$$

Where Φ_{nom} is the nominal magnetic flux, V_{nom} is the nominal voltage, and ω_{nom} is the angular velocity.

$$\Phi = \phi_{pu} \times \Phi_{nom} \quad (2)$$

Where ϕ_{pu} is the magnetic flux per unit value, and Φ is the total magnet flux.

The nominal power of a round rotor PMSG is given the following Equation:

$$P_{nom} = \sqrt{3} V_{nom} I_{nom} \quad (3)$$

Where P_{nom} is the nominal round rotor power, I_{nom} is the nominal current. The nominal impedance of the round rotor PMSG is determined as follows:

$$Z_{nom} = \frac{\sqrt{3} V}{3 I_{nom}} \quad (4)$$

$$R_s = R_{spu} Z_{nom} \quad (5)$$

Where R_{spu} is the resistance per unit value, and Z_{nom} is the nominal impedance.

The inductance of the round rotor PMSG dq0 frame L_{dq} is expressed as follows:

$$L_{dq} = L_{dq_pu} \times L_{nom} \quad (6)$$

Where L_{dq_pu} is the inductance per unit value.

The moment of inertia of the round rotor is given by the Eq. 7:

$$J = \frac{2 N_p H P_{nom}}{\omega_{nom}} \quad (7)$$

Where J is the inertia moment, N_p is the number of pole pairs, and H is the inertia constant.

Aerodynamic of Wind Turbine

The wind flowing through the rotor blades at the speed rate is converted into kinetic energy (Zhao and Ding, 2018). The kinetic power equation is expressed by the following expression (Abad et al., 2011; Letcher, 2017):

$$P_M = \frac{1}{2} C_p(\lambda, \beta) \rho \pi R^3 v_{rated}^3 \quad (8)$$

Where R is the radius of the rotor, ρ is the air density, v_{rated} is the wind velocity, λ is the tip ratio, β is the blade pitch angle, and C_p is the wind power coefficient.

The Equation of the torque T_t is expressed as [14]:

$$T_t = \frac{\rho \pi R^3 v^2}{2 \lambda} \quad (9)$$

Therefore, for the modelling of the Matlab Simulink system, the parameter used is given in Table 1.

Table 1 Generator and aerodynamic modelling parameters.

Parameter	Value	Parameter	Value
P_n	1.53 MW		35000 kgm ²
P_n	953 V	N	48
R	0.027	P_n	6.542 rad/sec
R	0.006Ω	H	5.005
L_{-}	0.5131	P_M	1.6 MW
L	0.000395 H	T_t	1.4.105 Nm
N	1.18842	$C_p(\lambda, \beta)$	0.34
P_n	2.4768 Wb	ρ	1.12
	1.48 Wb	R	33.05 m
Ω_R	0.4	v_{rated}	13.36 m/s

Modelling of PWM Rectifier

The PWM rectifier schematic is depicted in Figure 2. It is a three-phase regenerative rectifier based in a voltage source converter and consists of a line inductance on the AC side (L_s, R_s), six individual IGBT switches, and a DC-link capacitor on the DC side. The rectifier receives AC power from a balanced three-phase voltage source (V_a, V_b , and V_c), and the current supplied are I_{ra}, I_{rb} and I_{rc} . The DC output of the rectifier provides a current I_{dc} to an RL load and the large-scale system storage. The three-phase voltage source rectifier in the abc coordinates is given by the following equations (Acikgoz *et al.*, 2016; Brito *et al.*, 2015):

$$\begin{bmatrix} L_s \frac{dI_{ra}}{dt} \\ L_s \frac{dI_{rb}}{dt} \\ L_s \frac{dI_{rc}}{dt} \\ L_s \frac{dI_{dc}}{dt} \end{bmatrix} = \begin{bmatrix} -R_s & 0 & 0 & 0 \\ 0 & -R_s & 0 & 0 \\ 0 & 0 & -R_s & 0 \\ S_c & -1 & 0 & 0 \end{bmatrix} \begin{bmatrix} I_{ra} \\ I_{rb} \\ I_{rc} \\ I_L \end{bmatrix} + \begin{bmatrix} - \\ - \\ S_b \\ 0 \end{bmatrix} \begin{bmatrix} V_{ra} \\ V_{rb} \\ V_{rc} \\ V_{dc} \end{bmatrix} \quad (10)$$

Where V_{ra}, V_{rb} and V_{rc} are the rectifier input voltages expressed as a function of switching devices, and S_a, S_b and S_c are the switching functions, either 0 (switch is off) or 1 (switch on).

$$V_b = \begin{cases} V_a = V_m \sin \theta \\ V_m \sin \left(\theta - \frac{2\pi}{3} \right) \\ V_c = V_m \sin \left(\theta + \frac{2\pi}{3} \right) \end{cases} \quad (11)$$

Using Park's transformation, the model PWM rectifier equation is expressed as:

$$\begin{bmatrix} V_d \\ V_q \end{bmatrix} = L_s \begin{bmatrix} \frac{dI_d}{dt} \\ \frac{dI_q}{dt} \end{bmatrix} + \begin{bmatrix} R_s & -\omega L_s \\ \omega L_s & R_s \end{bmatrix} \begin{bmatrix} I_d \\ I_q \end{bmatrix} + \begin{bmatrix} V_{rd} \\ V_{rq} \end{bmatrix} \quad (12)$$

Where V_d and V_q , V_{rd} and V_{rq} , and I_d and I_q are the voltage V_a, V_b and V_c , the voltage V_{ra}, V_{rb} and V_{rc} , and the current I_{ra}, I_{rb} and I_{rc} in dq frame respectively, and $\theta = \omega t$ is the angle between the d-axis and qaxis.

By transforming the Eq.13 into d-q rotating reference frame, the Equation will become (Chen and Jin, 2006).

$$V^d = \begin{cases} \frac{di^d}{dt} \\ L_s \frac{di^d}{dt} + \omega L_s i^q + u^d \end{cases} \quad (13)$$

$$0 = L_s \frac{di^q}{dt} - \omega L_s i^d + u^q$$

Where the resistance value is neglected as it is very small and $V_q = 0$.

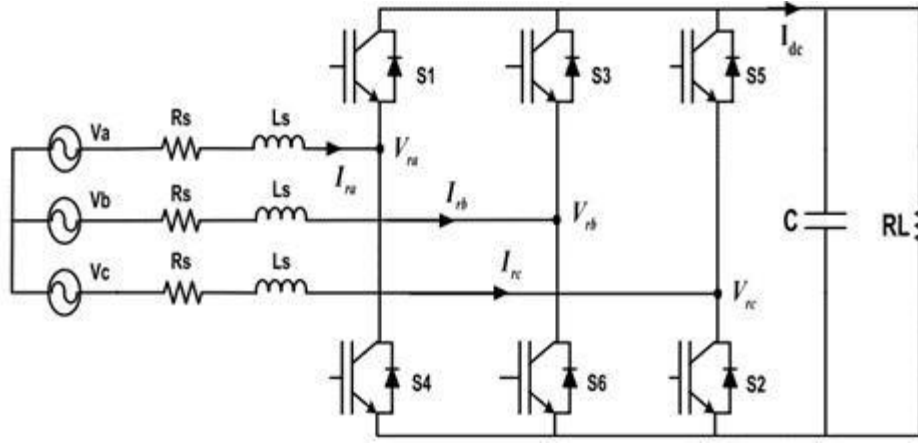


Figure 2 Two level rectifier voltage source topology. [16]

Modeling Line Inductance

The inductance has a major role in the rectifier operation as it generates an induced voltage which makes the voltage source rectifier to operate in boost mode and allows the DC-link voltage to be higher than the magnitude of the input voltage by blocking the diodes for a proper operation of the system. In addition, the inductance also operates as a filter to reduce the current ripple and the operation range of the rectifier at the same time (Chen and Jin, 2006). The voltage drop across the inductance controls the current, and this voltage is controlled by the rectifier, although its highest value is limited by the DC-link voltage (Marian et al., 2002). The inductance can be determined using Eq.14 as follows (Wang et al., 2013):

$$L_s \geq \frac{2V_{dc}\Delta I_{max}}{(2V_{dc}-3E_m)E_m T_s} \quad (14)$$

Where ΔI_{max} is the maximum ripple current generally chosen as 20% of the maximum current, E_m is the peak voltage of the AC generator, and T_s is the sampling period.

Modelling the DC-link Voltage

A proper operation of the rectifier depends on the minimum DC-link voltage, which is generally determined by the peak of line to line voltage given in Eq.15 as follows (Marian et al., 2002):

$$V_{DC-min} \geq \frac{2\sqrt{2}}{\sqrt{3}} V_{LN(peak)} = \frac{2\sqrt{2}}{\sqrt{3}} V_{LN(rms)} = 1.663 V_{LL(peak)} \quad (15)$$

Where V_{DC-min} is the minimum DC-Link and $V_{LN(rms)}$ is the line to ground voltage.

The DC-link capacitor can be determined using the following Equation:

$$C_{DC} = \frac{P}{2\pi f V_{DC} \Delta V_{DC}} \quad (16)$$

Where ΔV_{DC} is the maximum ripple DC voltage and it is usually 5% of the supply voltage, V_{DC} is the DC bus voltage, P is the active power, and f is the generator frequency.

The PWM rectifier modelling parameter is given in the Table 3.

Table 2 PWM rectifier modelling parameters.

Parameter	Value
	1150 Volts
	953 Volts
	0.005 Ω
	0.0885 F
	4.14x10 ⁻³ H

Control System

This study's adopted control is based on a voltage-oriented control strategy (VOC), and it is shown in Figure 3. The schematic consists of a fast-dynamic response and aims to control the output voltage using a current double loop structure. The outer loop is a DC-link voltage control that produces the inner current references.

Outer Loop Control

The outer loop control maintains the DC-link voltage value close to a set DC reference voltage, which must be higher than the generator peak voltage to keep the diode of the converter blocked. When this condition is satisfied, the outer loop control maintains the DC-link voltage value close to a set DC reference voltage, which must be higher than the generator peak voltage to keep the diode of the converter blocked. Then the DC-link voltage is measured and compared to the set DC reference. The error obtained from the comparison is used to generate the reference i_d^* current for the current loop through a PI controller (Chen and Jin, 2006). The tuning parameters can be estimated as follows (Teodorescu et al., 2011).

$$\begin{cases} k_{pv} = 0.12 T_s \\ T_{iv} = 17T \end{cases} \quad (17)$$

Where k_{pv} is the proportional gain, T_{iv} the time integrator in the outer voltage loop, T_s is the sampling period given by:

$$T_s = \frac{1}{f_s} \quad (18)$$

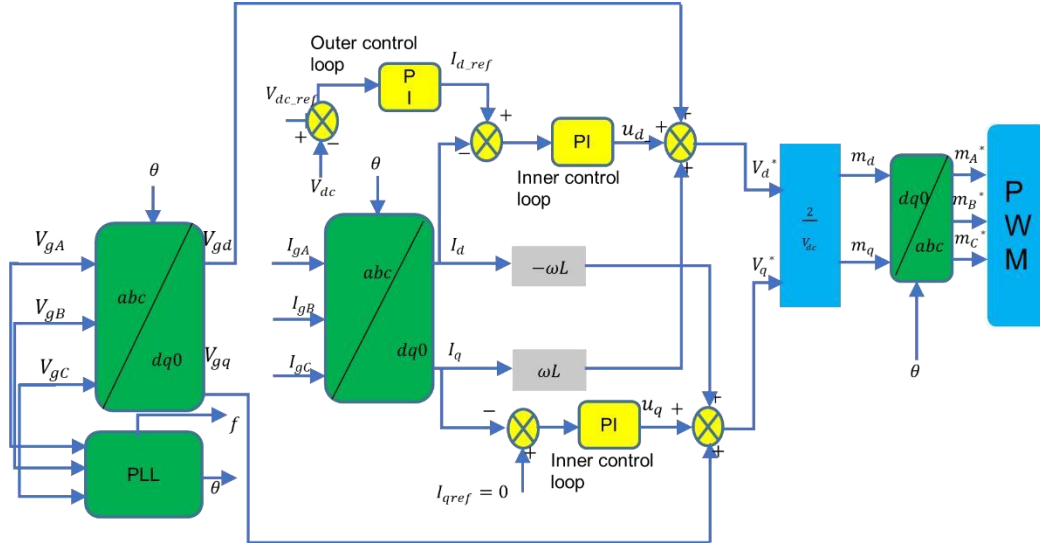


Figure 3 Control system schematic.

Inner Loop Control

In the inner loop, the current i_d and i_q obtained through the dq0 transformation of the generator current (I_a , I_b and I_c) are compared respectively with the i_{d_ref} generated at the outer loop and i_{q_ref} which is set to zero (Pashaei and Aydemir, 2014). The inner loop tuning parameter used in this study are estimated through the following Equation (Teodorescu et al., 2011):

$$\begin{cases} k_{pi} = 3T_s \\ T_{ii} = R_s \end{cases} \quad (19)$$

Where k_{pi} is the proportional gain and T_{ii} is the integration time constant of the inner loop control.

The tuning parameters of both the outer and the inner loop are given in the Table 3.

Modulation Control

The modulation signals m_d^* and m_q^* are used to generate the PWM signals to drive the rectifier switches based on the following Equation (Esmailian et al., 2014):

$$m_d^* = \begin{cases} \frac{v_{2DC}}{V_{DC}} (V_{gd} + L_s \omega I_q + u_d) \\ m_q^* = \frac{v_{2DC}}{V_{DC}} (V_{gq} - L_s \omega I_d + u_q) \end{cases} \quad (20)$$

Where L_s and ω are the disturbances from input power transmission, and u_d and u_q are the current errors output signals.

Modelling Phase Locked Loop (PLL)

The Phase-Locked Loop (PLL) is used in this study to generate the phase angle for the transformation. A typical PLL circuit consists of the phase detector, the loop filter, and the voltage controlled oscillator (Behera and Thakur, 2016). The closed-loop transfer function of a PLL (Figure 4) is given by the following equation (Timbus et al., 2005):

$$G_{PLL}(S) = \frac{\theta^*}{\epsilon} = \frac{K_1 + \frac{K_2}{s}}{s^2 K_1 + s K_2 + K_1} \quad (21)$$

Where K_1 is the PI loop filter proportional and K_2 is the proportional corresponding integral gain.

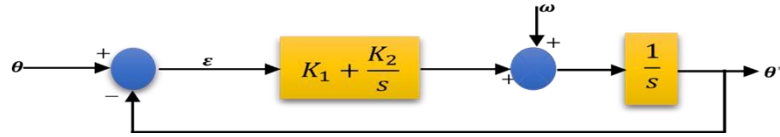


Figure 4 Small signal mode (Behera and Thakur, 2016).

The parameters K_1 and K_2 of a PLL can be evaluated using the following expression (Teodorescu et al., 2011):

$$\begin{cases} \omega_n = \sqrt{K_2} \\ \zeta = \frac{K_1}{\sqrt{K_2}} \end{cases} \quad (22)$$

Where ω_n is the natural frequency and ζ is the damping ratio.

Table 3 provides the determined values of ω_n and ζ .

Table 3 Tuning parameters inner, outer loop and PLL.

Outer	Value	Inner	Value	Parameter	Value
K_{pv}	49.35	K_{pi}	0.3497	K_1	1
T_{iv}	2.81 ms	T_{ii}	64.13 ms	K_2	356

Results and Discussion

A simulation was carried out to analyse the performance of the model depicted in Figure 1 for a simulation time of about 20 seconds based on parameters from Table 1 to Table 4.

It is considered that the wind generator produces AC power at a constant wind speed of 13 m/s. The wind generator has a power rating of 1.53 MW with a phase to phase voltage of 953 V at 50 Hz. The power obtained at the wind generator's output terminals is rectified to feed a DC load connected at the output terminals of the rectifier. The rectifier's output power delivers DC power of a magnitude of 1.26 MW at 1150 V; hence, the rectifier efficiency is around 82 %. The control approach used to regulate the rectifier's output parameters is based on the closed-loop voltage-oriented strategy, as shown in Figure 3. The control

method consists of keeping the DC output voltage as close as possible to the adopted reference DC voltage of 1150 Volts through proportional-Integral controllers. The control strategy includes two control loops, namely the outer and the inner control loops. In this case, the outer control loop is the DC-link voltage control that aims to generate the inner current in dq0 reference. The inner control loop uses the error between the dq0 reference current generated by the outer control loop and the system currents. The error is then used in the inner PI controller to produce the modulation signal in dq0 frame. Then, the inner control loop output in dq0 is transformed back to the abc frame to obtain the modulation in the abc frame to generate the Pulse Width Modulation signals to drive the rectifier. The simulation results are presented in three sections: the AC, control scheme, and DC side results. The AC section focuses on the PMSG voltage, current, and active and reactive power and the output voltage, current, and active and reactive power. The control scheme discusses the obtained PWM signals, whereas the DC side deals with the DC-link voltage and voltage, current and power at the load side.

AC Side Results

For a rated wind velocity of about 13 m/s, the wind generator's active and reactive power obtained from the simulation are shown in Figure. 5. The average active power value is around 1.5 MW (Figure. 5a-active power), while the reactive power is 403 kW (Figure. 5b-reactive power). Between 0 and 3 seconds, the simulation results display an overshoot and undershoot for the active and reactive power signals, respectively, as the system did not reach its stability yet. However, after 3 seconds, it can be seen both signals gain their stability. The phase to ground voltage and the phase current at the wind generator's output terminals are depicted in Figures 5c and 5d. The RMS voltage value is around 549 V (Figure. 5cDC bus voltage), while the RMS of the phase to phase voltage is around 951 Volts. On the other hand, this generator's phase current is about 1082 Amps (Figure 5d- current bus). Both signals exhibit harmonics higher than the adopted system frequency of 50 Hz.

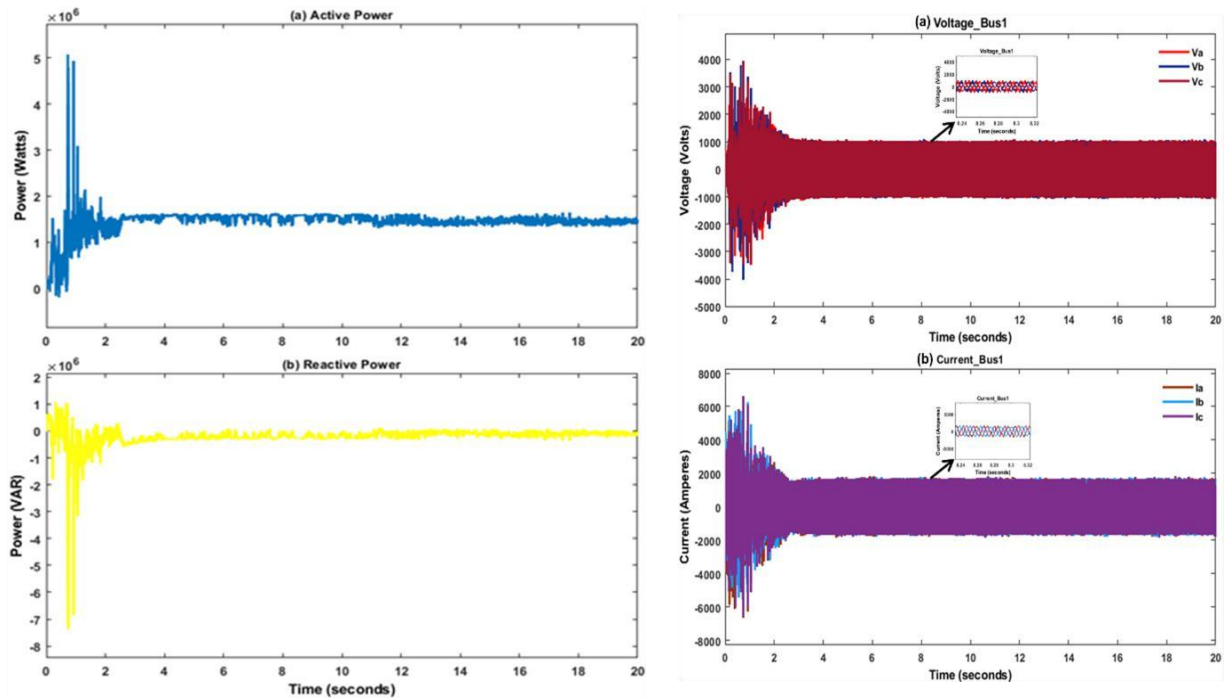


Figure 5 (a) Active Power and (b) Reactive power of the wind generator; c) Voltage and (d) current curves of the wind generator.

The phase to ground voltage wave is characterised by a Total Harmonics Distortion of 141.38% (Figure. 6a), whereas the phase current signal shows a Total Harmonics distortion of 13.54% (Figure 6b).

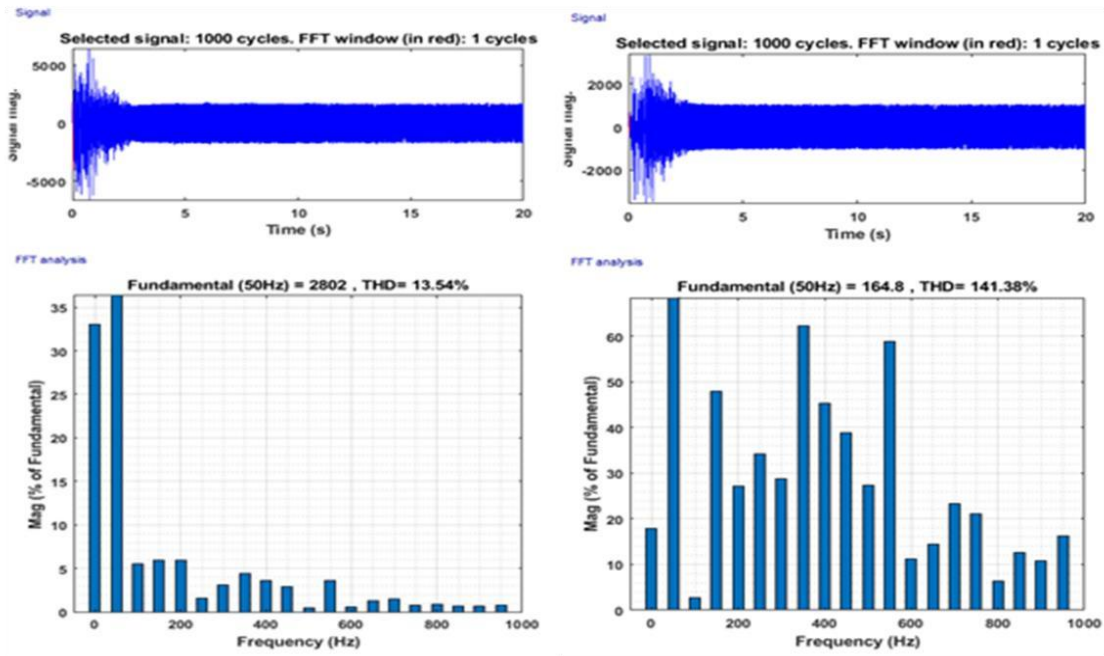


Figure 6 (a)Voltage and (b) Current Total Harmonics Distortion.

Results of the DC Side

The DC side results consist of comparing the DC voltage of the rectifier against the DC reference voltage and assessing the rectifier's performance when its output is connected terminal to an R load, RL load, and RC load. Figure 7 compares the DC voltage and the DC reference voltage used in the control loop. The reference voltage is set to 1150 V, and at the steady-state, both the DC voltage and the DC reference voltage are approximately equal. The DC voltage has a rise time of about 2.599 seconds, which is required for the voltage to rise from 0 to 100 % of its final value. Furthermore, the overshoot and undershoot at the start of the signal are 0.505 % and 2 %, respectively.

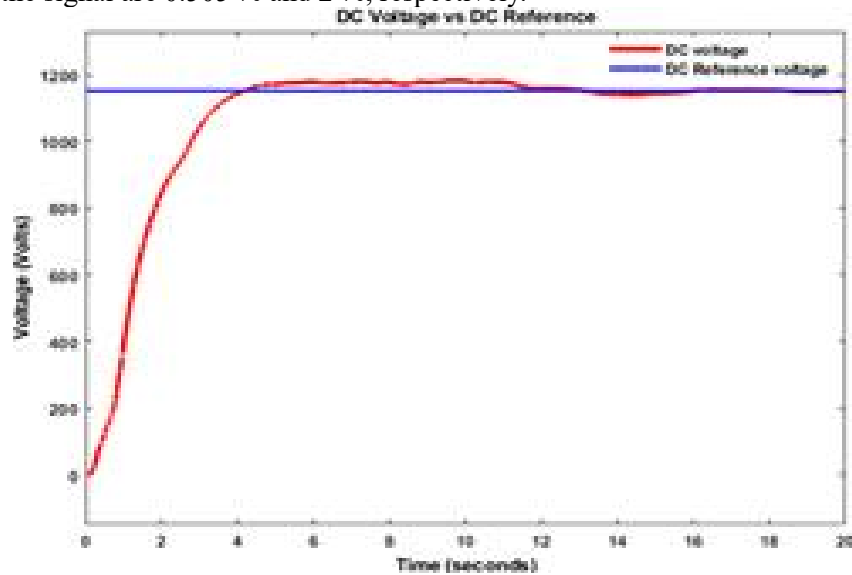


Figure 7 DC Voltage versus DC Reference voltage.

Case Study

A load of impedance equals 1.02Ω , consisting of resistance of 1.02Ω and inductance of 1 Henry, which may represent an asynchronous motor. The voltage and current supplying the load are shown in Figure 14. From the beginning of the simulation, it can be observed that the voltage signal has oscillations until it

reaches its stability and settles at 1105 V (Figure 8a), while the current shows less oscillation until it gets 1162 Amps (Figure 8b). The voltage signal shows an overshoot of 11.798 %, while the undershoot is 18.964 %, and its rise time is 1.277 seconds. On the other hand, the current signal displays an overshoot of 0.505 %, while the undershoot is 3.25 %, and the rise time is 3.833 seconds. The resulting power measured at the load side is shown in Figure 8c; this power oscillates between 0 seconds to about 16 seconds until it gets to apparent stability of around 17 seconds. The measured power value is 1.207 MW, slightly lower than the power in case of a resistive load.

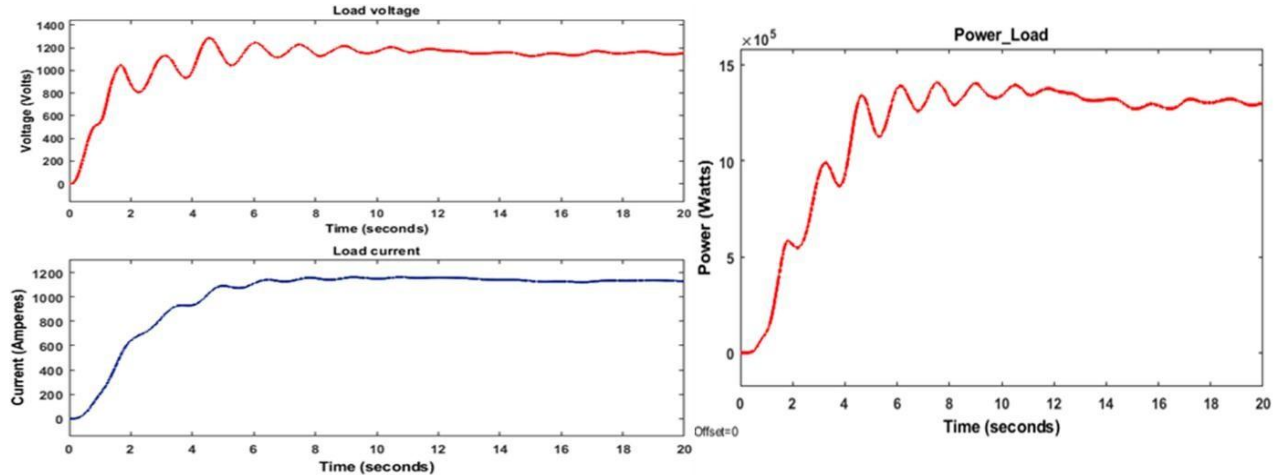


Figure 8 Voltage and Current of an RL load; Power supplied to RL load.

Conclusion

A renewable microgrid is the combination of electrical loads and micro sources functioning as one system that can operate in two modes one connected to a larger power grid, and the other one can be totally in the islanded way. The microgrids based on renewable energy solve energy problems locally, ensure energy security, and increase system flexibility. This study focused on developing PWM rectifier control for large-scale energy storage in a renewable microgrid. The system results consisted of a three-phase PWM rectifier receiving AC power from a 1.53 MW permanent magnet synchronous wind generator at a line voltage of 953 V. The rectifier delivered 1.26 MW at a DC voltage of 1150 V to a DC load connected to its output terminals. The control system scheme adopted in this study was based on a voltage-oriented control strategy. The modelling and simulation were carried out using Matlab/Simulink environment. An RL was considered to evaluate the performance of the designed controller. The results showed a good performance of the designed controller as the output voltage could be maintained close to the set reference value.

References

- Abad, G., Lopez, J., Rodriguez, M.A. and Iwanski, G. (2011), Doubly Fed Induction Machine, John Wiley & Sons, Inc, New Jersey.
- Acikgoz, H., Kececioglu, O.F., Gani, A., Yildiz, C. and Sekkeli, M. (2016), "Improved Control Configuration of PWM Rectifiers based on Neuro - Fuzzy Controller", SpringerPlus, Springer International Publishing, Vol. 5 No. 1, pp. 1–19, doi: 10.1186/s40064-016-2781-5.
- Arbab-Zavar, B., Palacios-Garcia, E.J., Vasquez, J.C. and Guerrero, J.M. (2019), "Smart inverters for microgrid applications: A review", *Energies*, Vol. 12 No. 5, doi: 10.3390/en12050840.
- Behera, R.R. and Thakur, A.N. (2016), "An Overview of Various Grid Synchronization Techniques for SinglePhase Grid Integration of Renewable Distributed Power Generation Systems", *International Conference on Electrical, Electronics, and Optimization Techniques, ICEEOT 2016*, IEEE, Chennai, pp. 2876–2880, doi: 10.1109/ICEEOT.2016.7755223.
- Binder, A. and Schneider, T. (2005), "Permanent Magnet Synchronous Generators for Regenerative Energy Conversion - A Survey", *IEEE*, p. 10.
- Brito, R., Carvalho, A. and Gericota, M. (2015), "A New Three-Phase Voltage Sourced Converter Laplace Model", *Proceedings - 2015 9th International Conference on Compatibility and Power Electronics, CPE 2015*, IEEE, pp. 160–166, doi: 10.1109/CPE.2015.7231066.

- Caixeta, D.A., Guimarães, G.C. and Chaves, M.L.R. (2014), “Modeling of a Wind Energy Conversion System for Dynamic Analysis Using Alternative Transients Program”, *Ciencia and Engenharia/Science and Engineering Journal*, Vol. 23 No. 1, pp. 37–45, doi: 10.14393/19834071.2014.26547.
- Chen, Y. and Jin, X.M. (2006), “Modeling and Control of Three-Phase Voltage Source PWM Rectifier”, *Conference Proceedings - IPEMC 2006: CES/IEEE 5th International Power Electronics and Motion Control Conference*, Vol. 3, pp. 1459–1462, doi: 10.1109/IPEMC.2006.297317.
- Ellabban, O., Abu-Rub, H. and Blaabjerg, F. (2014), “Renewable Energy Resources: Current Status, Future Prospects and Their Enabling Technology”, *Elsevier Renewable and Sustainable Energy Reviews*, Elsevier, Vol. 39, pp. 748–764, doi: 10.1016/j.rser.2014.07.113.
- Esmacilian, H.R., Fadaeinedjad, R. and Moschopoulos, G. (2014), “Dynamic operation and Control of a Stand-Alone PEM Fuel Cell System”, *Conference Proceedings - IEEE Applied Power Electronics Conference and Exposition - APEC*, pp. 3378–3384, doi: 10.1109/APEC.2014.6803792.
- Frisfelds, K. and Krievs, O. (2019), “Design of a three-phase bidirectional PWM rectifier with simple control algorithm”, *Latvian Journal of Physics and Technical Sciences*, Vol. 56 No. 3, pp. 3–12, doi: 10.2478/lpts-2019-0015.
- Hannachi, M. and Benhamed, M. (2017), “Modeling and Control of a Variable Speed Wind Turbine with a Permanent Magnet synchronous Generator”, *IEEE 2017 International Conference on Green Energy Conversion Systems (GECS)*, No. 1.
- Khaburi, D.A. and Nazempour, A. (2010), “Design and Simulation of a PWM Rectifier Connected to a PM Generator of Micro Turbine Unit”, *Scientia Iranica*, Elsevier B.V., Vol. 19 No. 3, pp. 820–828, doi: 10.1016/j.scient.2011.09.017.
- Kondylis, G.P., Vokas, G.A., Anastasiadis, A.G. and Konstantinopoulos, S.A. (2017), “Application of Voltage Oriented Control Technique in a Fully Renewable, Wind Powered, Autonomous System with Storage Capabilities”, *AIP Conference Proceedings*, Vol. 1814, doi: 10.1063/1.4976285.
- Letcher, T.M. (2017), *Wind Energy Engineering A Handbook for Onshore and Offshore Wind Turbines*, edited by Letcher, T.M., Elsevier, London.
- Marian, K.P., Blaabjerg, F. and Krishnan, R. (2002), *Control in Power Electronics*, edited by Irwin, J.D.
- Pashaei, A. and Aydemir, M.T. (2014), “Design and Implementation of a Pulse Width Modulated Rectifier for Industrial Applications”, *22nd Iranian Conference on Electrical Engineering, ICEE 2014*, pp. 574–579, doi: 10.1109/IranianCEE.2014.6999608.
- Planas, E., Andreu, J., Gárate, J.I., Martínez De Alegría, I. and Ibarra, E. (2015), “AC and DC Technology in Microgrids: A review”, *Renewable and Sustainable Energy Reviews*, Vol. 43, pp. 726–749, doi: 10.1016/j.rser.2014.11.067.
- Qiang, L., Libin, Y., Liangyu, M., Weiliang, L. and Yinsong, W. (2015), “Modeling and Control of Wind/PV/Battery Micro-grid Based on Matlab/Simulink”, *International Conference on Information Technology and Management Innovation (ICITMI)*, pp. 891–895.
- Stephen, A.A. (2017), *Assessment of Renewable Energy*, University of Cape Town.
- Teodorescu, R., Liserre, M. and Rodriguez, P. (2011), *Converters for Photovoltaic and Wind Power Systems*, John Wiley & Sons, Inc.
- Thorpe, D. (2015), “New Study Identifies How Cities Can Cut Energy Use by 25% by 2050”, *The Sustainable Cities Collective*, available at: <https://www.smartcitiesdive.com/ex/sustainablecitiescollective/newstudy-identifies-how-cities-can-cut-energy-use-25-2050/1036406/> (accessed 4 March 2019).
- Timbus, A., Teodorescu, R., Blaabjerg, F. and Liserre, M. (2005), “Synchronization Methods for Three Phase Distributed Power Generation Systems. An Overview and Evaluation”, *PESC Record - IEEE Annual Power Electronics Specialists Conference*, Vol. 2005, IEEE, pp. 2474–2481, doi: 10.1109/PESC.2005.1581980.
- Wang, X., Yu, J., Bai, B. and Chen, D. (2013), “Parameter Analysis and Calculation of Inductor for PWM Rectifier”, *Proceedings - 2013 International Conference on Mechatronic Sciences, Electric Engineering and Computer, MEC 2013*, Institute of Electrical and Electronics Engineers Inc., pp. 3822–3826, doi: 10.1109/MEC.2013.6885655.
- Yusoff, N.A., Razali, A.M., Karim, K.A., Sutikno, T. and Jidin, A. (2017), “A Concept of Virtual-Flux Direct Power Control of Three-Phase AC-DC Converter”, *International Journal of Power Electronics and Drive Systems*, Vol. 8 No. 4, pp. 1776–1784, doi: 10.11591/ijpeds.v8i4.pp1776-1784.
- Zhao, Y. and Ding, C. (2018), “Wind Power Generator Output Model Based on the Statistical Wind Speed Distribution Derived From the Historical Data”, *2018 2nd IEEE Conference on Energy Internet and Energy System Integration (EI2)*, IEEE, pp. 1–5.